Geometric and electronic structure of antimony on the GaAs(110) surface studied by scanning tunneling microscopy

P. Mårtensson and R. M. Feenstra
IBM Research Division, Thomas J. Watson Research Center, P.O. Box 218, Yorktown Heights, New York 10598
(Received 1 September 1988; revised manuscript received 31 October 1988)

Antimony overlayers on the GaAs(110) surface have been studied by scanning tunneling microscopy and spectroscopy. The Sb is observed to grow as a 1×1 ordered monolayer. The positions of the Sb atoms in the surface unit cell are deduced from voltage-dependent imaging, and compared with previously proposed structural models. A best fit is found for a model in which the Sb atoms occupy positions similar to what would be the positions of Ga and As atoms at an unrelaxed GaAs(110) surface, in agreement with the results from low-energy electron-diffraction experiments. The surface-state density is measured with tunneling spectroscopy. Two filled-state peaks and one empty-state peak are observed in the spectra, as well as a band-gap region with a width nearly equal to the bulk band gap. These observations are compared with previous photoemission results and theoretical calculations.

I. INTRODUCTION

Because of the great practical importance of Schottky-barrier formation at metal-semiconductor interfaces, the adsorption of metal atoms on semiconductor surfaces has been the subject of numerous experimental and theoretical studies.[1] One of the more extensively studied systems is antimony on GaAs(110).[2–15] Early work by Skeath *et al.*[2] using low-energy electron diffraction (LEED) and photoemission showed that room-temperature deposition of one monolayer (ML) (Ref. 16) of Sb on clean GaAs(110) results in a stable and ordered (1×1) adsorbate structure. Core-level spectroscopy indicated the existence of at least two chemically distinct Sb species at the surface, while valence-band spectrosopy revealed Sb-induced surface states just below the GaAs valence-band maximum (VBM).[2] Results from LEED and Auger-electron–spectroscopy (AES) experiments by Carelli and Kahn[3] indicated that the Sb overlayer is formed through a lateral growth of ordered 1-ML-high islands. Desorption experiments by the same authors show that the ordered Sb overlayer is stable up to temperatures of $\sim550\,^{\circ}\mathrm{C}$, whereas any excess Sb desorbs at temperatures as low as $\sim250\,^{\circ}\mathrm{C}$.[3]

Duke *et al.*[4] have studied the atomic structure of the GaAs(110)1×1-Sb surface in an extensive dynamical LEED-intensity analysis of several classes of models. The most satisfactory description of the experimental LEED data was obtained for a model in which zigzag chains of Sb atoms bridge the chains of Ga and As atoms on a nearly unrelaxed GaAs(110) substrate, as shown in Fig. 1. For this type of geometry, originally proposed by Skeath *et al.*,[2] there are two inequivalent Sb atoms per surface unit cell, one bonded to As and the other to Ga.

So far, two groups have calculated the surface-electronic structure of GaAs(110)1×1-Sb. Bertoni *et al.*[5] performed a self-consistent pseudopotential calculation using the optimal structural parameters as determined by Duke *et al.*,[4] while Mailhiot *et al.*[7] performed an empirical tight-binding calculation for an energy-minimized surface geometry of the same type. The calculations indicate the existence of filled surface states just below the VBM, in agreement with early photoemission results,[2,6,8] in addition to several lower-lying filled states, as well as empty states near the conduction-band minimum (CBM). More recently, the dispersion of four filled and one empty surface-state band have been determined with angle-resolved photoemission[10,11] and inverse photoemission.[15] The experimentally determined dispersions show a qualitative agreement with the results from the surface band-structure calculations,[5,7] providing additional support for the chain model shown in Fig. 1. It should be noted, however, that no calculations have been reported for any of the other models that have been suggested.[2–4]

Since the Sb/GaAs(110) system is well characterized

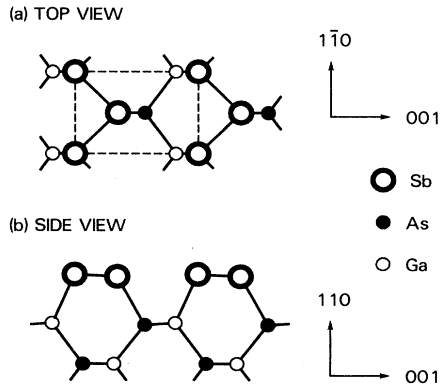

FIG. 1. Schematic diagram of the surface geometry for GaAs(100)1×1-Sb as determined by LEED (Ref. 4). (a) Top view. (b) Side view.

and relatively simple, it is well suited for studies of Ferm-level pinning, band bending, and Schottky-barrier formation. There has, however, been some controversy in the literature regarding the amount of band bending at the GaAs(110)1×1-Sb surface. Work-function measurements[8] have resulted in a value of ~0.6 eV for the band bending at 1 ML coverage of Sb on both *n*- and *p*-type GaAs, while surface-photovoltage[9] and Raman-scattering[12] experiments on *n*-type GaAs have indicated that an initial band bending that occurred for submonolayer coverages was removed for a coverage of 1 ML. Recently, Schäffler *et al.*[14] studied the influence of thermal annealing on band bending and surface quality using high-resolution core-level spectroscopy. They showed that room-temperature deposition of Sb leads to a partly disordered overlayer with a large Schottky barrier as compared to surfaces that were annealed at 330 °C. These results were confirmed in the inverse-photoemission experiment by Drube and Himpsel.[15]

In a recent paper[17] we presented a scanning-tunneling-microscopy (STM) study of submonolayer coverages of Sb on GaAs(110) in which we directly observed the spectrum of states responsible for the Fermi-level pinning at the Sb/GaAs(110) surface. These states were shown to be spatially localized near the edges of Sb islands. In the present paper we focus on the atomic and electronic structure of the Sb overlayer itself. Using voltage-dependent imaging, we obtain information about the registration of the two inequivalent Sb atoms with respect to the underlying GaAs lattice. A comparison with previously proposed models[2–4] shows that the chain model in Fig. 1 gives the best agreement with our STM data. Using tunneling spectroscopy we determine the energy positions of filled and empty surface states, obtaining good agreement with available photoemission[10,11] and inverse-photoemission[15] data. A new spectroscopic method is used here, which enables us to obtain the entire spectrum, in a single scan, with high dynamic range. The normalization of the conductivity spectrum is discussed, and a method is introduced which overcomes some difficulties associated with large band-gap regions in the spectra.

II. EXPERIMENTAL DETAILS

This work was performed with two tunneling microscopies, one of which has been described previously.[18] The second microscope has a similar design, and is incorporated in an ultrahigh-vacuum system with facilities for LEED and AES, which were used to characterize the samples. Tungsten probe tips were prepared by electrochemical etching, and cleaned *in situ* by electron-bombardment heating. GaAs(110) surfaces were prepared by cleaving *in situ* *p*-type wafers, doped with Zn at concentrations in the range $(1-4)\times10^{18}$ cm^{-3}. The orientation of the Ga and As dangling bonds on the clean surface was established by anisotropic etching techniques. With the samples at room temperature, high-purity antimony was deposited using either a filament-type evaporator or an effusion cell, with typical deposition rates of 0.2 and 0.05 ML/min, respectively. The total antimony coverages were estimated both from the STM images and using quartz-crystal thickness monitors assuming a sticking coefficient of unity. The background pressure in the vacuum chambers was better than 6×10^{-11} Torr, and the pressure never exceeded 2×10^{-10} Torr during evaporation with the filament, or 1×10^{-9} Torr during evaporation with the effusion cell.

All STM images shown here were recorded with a constant tunneling current of 100 pA. For most images the drift in the microscope was sufficiently low so that no drift correction to the data has been necessary. In those cases where a drift correction has been performed [Figs. 2(a), 2(b), 4, and 7], the drift rate was determined by comparing consecutive images. The crystallographic directions shown here in the images are all the same, with the $[\bar{1}10]$ axis oriented 45° counterclockwise from the horizontal. Voltage-dependent images were obtained by sequencing the sample voltage in the line scans to virtually eliminate drift effects between member images in a sequence.[19] Spectroscopy measurements were performed by the interrupted-feedback-loop method.[18,20] To build up a large dynamic range in the spectra, we move the probe tip towards the sample during the voltage sweep, thereby amplifying the current and conductivity. We use a continuous linear ramp in the tip-sample separation, moving the tip towards the surface as the magnitude of the voltage is reduced. The conductivity is measured with a lock-in amplifier, typically using 25 mV modulation at 1 kHz. The differential conductivity dI/dV is normalized to the total conductivity I/V in the manner described in Sec. III E.

III. RESULTS AND DISCUSSION

A. Overlayer growth

Figure 2 shows a series of STM images of the GaAs(110) surface with increasing Sb coverage. The GaAs substrate can be seen as the dark portions of the images, while the Sb-covered regions show up as the lighter portions. At very low coverages most of the GaAs substrate is bare, as can be seen in Fig. 2(a), which was obtained for a coverage of 0.03 ML. The periodic array of lines seen in this image represent the positions of the As atoms, since negative sample bias corresponds to tunneling from the filled states of the sample, which are mainly localized on the As atoms.[21] The antimony can be seen as separated protrusions of varying shapes and sizes. Even at the lowest coverages studied (0.02 ML) the protrusions are relatively large ($\gtrsim$10 Å width) and they seem to correspond to clusters of Sb atoms rather than to single atoms.

At 0.2 ML [Fig. 2(b)] the Sb clusters have started to grow together, forming flat terraces. The height of the terraces above the GaAs substrate, as observed in the STM images, is 2.5–2.8 Å, depending on the applied bias voltage.[22] As the coverage is increased to 0.7 ML [Fig. 2(c)] the Sb terraces coalesce, forming a continuous network extending over the entire GaAs surface. It is clear that the terraces are well ordered, although some protrusions formed by excess Sb on top of the terraces are al-

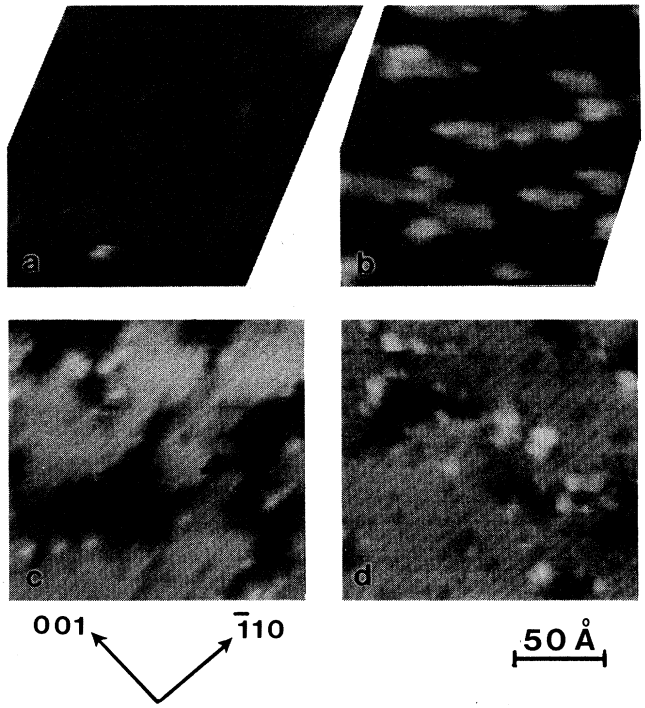

FIG. 2. STM images of GaAs(110) surfaces with increasing amounts of Sb. The coverages are (a) 0.03, (b) 0.2, (c) 0.7, and (d) 1.0 ML. The sample voltage was −2.5 V for images (a)–(c) and −2.0 V for image (d). The topographic height is displayed by a grey scale, ranging from 0 (black) to 6.5 Å (white).

ways present, as well as some small holes, which will be discussed further in Sec. III D. Due to the excess Sb there are some bare GaAs patches even at 1.0 ML coverage, as can be seen in Fig. 2(d). The excess Sb is present already at low coverages on small terraces, and since it is predominantly located at the terrace edges, most of it seems to be consumed in the growth process.

The above results show that, for submonolayer coverages, Sb grows laterally on GaAs(110), in 1-ML-high ordered patches, as deduced by Carelli and Kahn in their early LEED and AES study.[3] Due to the large size of the Sb clusters even at low coverages, it is not possible to determine the adsorption site of Sb on the GaAs(110) surface. However, it seems clear that there is no preferential bonding to either Ga or As atoms, except for possible effects at the edges of the growing Sb terraces. This is in contrast to a recent electron-energy-loss–spectroscopy study by Strümpler and Lüth,[13] in which a very rapid suppression of a Ga-characteristic excitonic transition was interpreted as evidence for a preferential bonding of Sb atoms to Ga sites. From our STM data we would expect that such a transition would show a linear decrease in intensity as a function of coverage, as was indeed observed in an earlier study by Li and Kahn.[9]

By counting the number of clusters in a large number of images, it is possible to estimate the density of adsorption sites for the Sb. For coverages of 0.02 ML we obtain a value of $(5.5\pm1.0)\times10^{12}$ cm^{-2}. This density of adsorption sites is larger than the average density of defects seen in images of the clean surface,[23] which is about 1×10^{12} cm^{-2}. This comparison suggests that defects do not play a major role in the adsorption of Sb on the GaAs(110) surface.

B. Overlayer structure

Figure 3(a) shows a high-resolution image of a surface covered with 1.0 ML antimony. In the ordered part of the Sb overlayer there is an array of topographic maxima separated by ~5.6 and ~3.9 Å in the [001] and [$\bar{1}$10] directions, respectively. These values are in good agreement with the size of the unit cell of the GaAs(110) surface, 5.65×4.00 Å^2, which means that only a single maximum per unit cell is seen in the image.

We have reproducibly observed a single topographic maximum per unit cell in all images obtained at large negative sample voltages, in the range −2 to −3 V. We associate this maximum with the dangling bond attached to one of the two Sb atoms in the unit cell, and conclude that the second atom is not imaged at large negative voltages. The fact that not all surface atoms are seen at some particular voltage is a feature of STM which commonly occurs on semiconductor surfaces. This feature arises from the fact that the images actually reveal the electronic states, and the various dangling bonds which compose

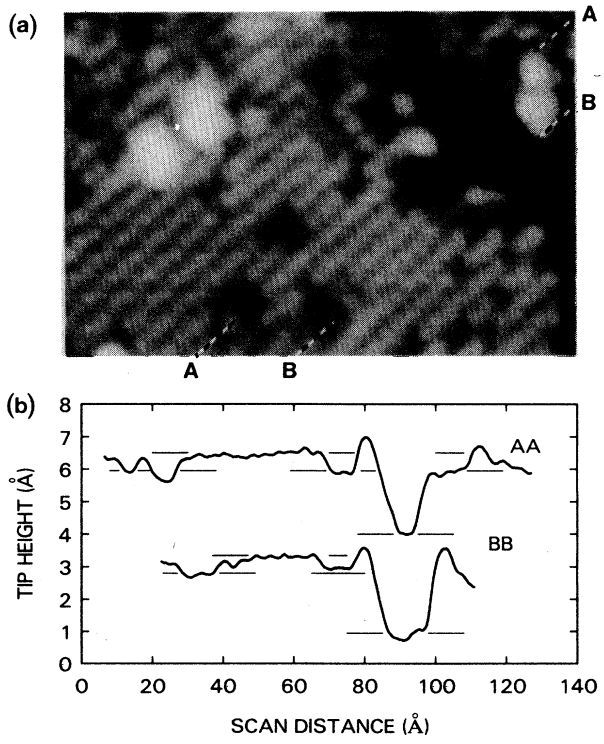

FIG. 3. (a) (120×90)-Å^2 STM image of antimony on the GaAs(110) surface, acquired with a sample voltage of −2.0 V. The Sb coverage is 1.0 ML. The topographic height is displayed by a grey scale, ranging from 0 (black) to 5 Å (white). (b) Cross-sectional cuts along the [$\bar{1}$10] direction, through the rows indicated in the image.

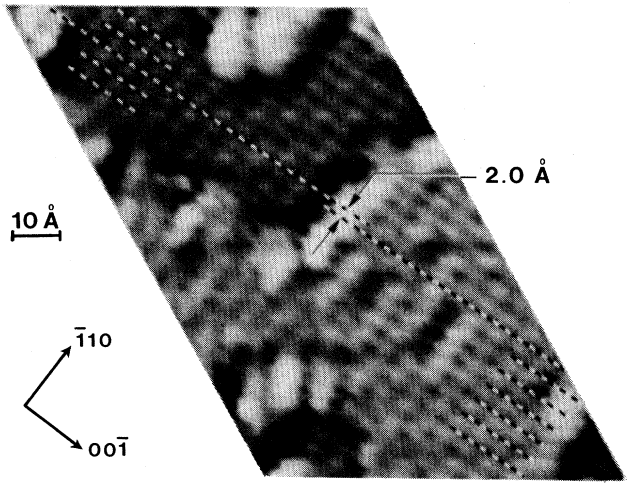

FIG. 4. STM image of the GaAs(110) surface covered with 0.7 ML Sb, acquired at a sample voltage of −2.0 V. The dashed lines are drawn through the minima of the [$\bar{1}$10] corrugation, showing the registration of the Sb atoms with respect to the substrate As atoms.

these states have amplitudes which are energy dependent. It is therefore necessary to study the dependence of the images on bias voltage to reveal the complete geometric structure of the surface.

The registration relative to the GaAs substrate of the Sb atom observed at large negative sample voltages is shown in Figs. 4 and 5. In the [$\bar{1}$10] direction, Fig. 4, we find a shift between the Sb maxima and the As maxima of 2.0 Å, which corresponds to 0.50 unit cell along this direction. Thus the Sb atoms are out of phase with the As atoms in this direction. Qualitatively, this out-of-phase relationship indicates that these Sb atoms are *not* bonded to the As atoms. Indeed, when we consider structural models in the following subsection, we find that these particular Sb atoms (seen at large negative voltages) are bonded to the Ga atoms of the substrate. We refer to this Sb atom as $Sb^{(Ga)}$. For the [001] direction, Fig. 5, we find a shift between the $Sb^{(Ga)}$ maxima and the As maxima of 2.6 Å, which corresponds to 0.46 unit cell along this direction.

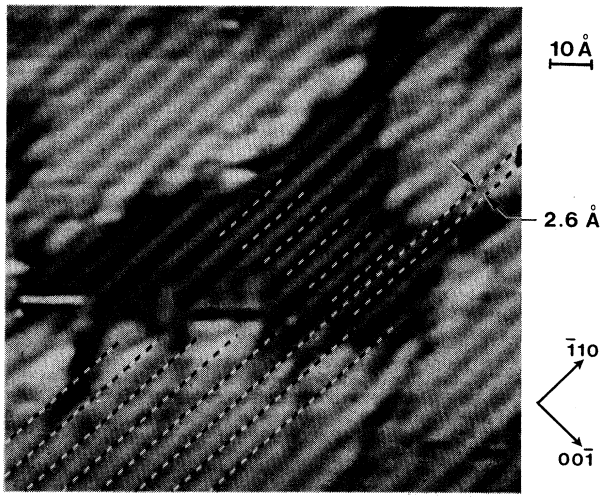

FIG. 5. STM image of the GaAs(110) surface covered with 0.7 ML Sb, acquired at a sample voltage of −2.5 V. The dashed lines are drawn through the minima of the [001] corrugation, showing the registration of the Sb atoms with respect to the substrate As atoms.

In Figs. 6(a)–6(c) we show three STM images of a well-ordered part of a Sb terrace, acquired simultaneously at sample voltages of −2.5, −2.0, and −1.5 V, respectively. The crosshairs are in identical locations in all images. The images acquired at −2.5 and −2.0 V are very similar, with rows extending in the [$\bar{1}$10] direction; there is no corrugation along this direction in these images. In the cross-sectional cuts shown in Fig. 6(d) it can be seen that the rows have a spacing close to 5.65 Å, which means that there is one row per unit cell, in agreement with the images in Figs. 3–5. We associate these rows with the $Sb^{(Ga)}$ atoms, and the lack of corrugation in the [$\bar{1}$10] direction is attributed to a probe tip which is blunt in that direction. In Fig. 6(c), acquired at −1.5 V, additional rows appear, located essentially midway between the original rows. We associate these additional

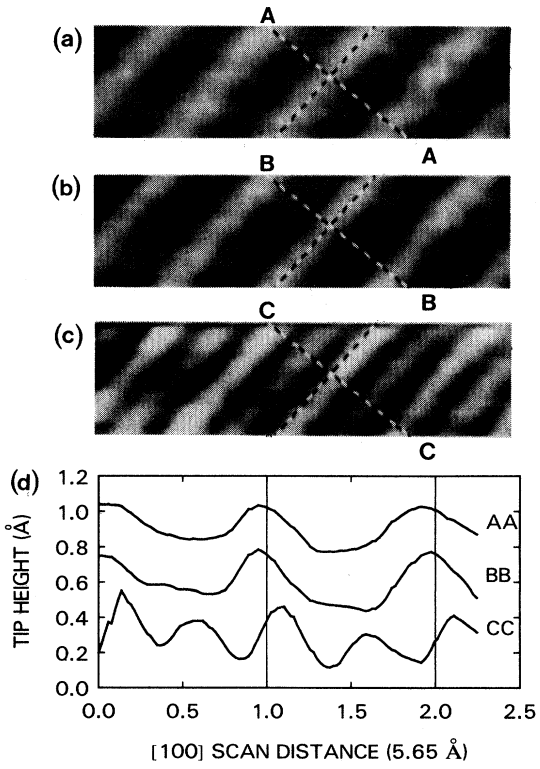

FIG. 6. (30×10)-Å^2 STM images of an ordered part of a Sb terrace acquired simultaneously at (a) −2.5, (b) −2.0, and (c) −1.5 V sample voltage. The crosshairs are located in identical positions in all images. The topographic height is displayed by a grey scale, ranging from 0 (black) to 0.5 Å (white). (d) Cross-sectional cuts along the [100] direction in images (a)–(c).

rows with the second Sb atom in the unit cell, $Sb^{(As)}$, which is bonded to an As atom in the substrate. The $Sb^{(As)}$ atoms are only observed at small negative voltages. In Fig. 7 an image acquired at -0.9 V is shown. Here, we again see two rows per unit cell extending in the $[\bar{1}10]$ direction, thus revealing both of the Sb atoms in the unit cell. The $Sb^{(Ga)}$ atoms are now resolved as individual maxima in the image, although the $Sb^{(As)}$ atoms still appear as rows without any corrugation along the $[\bar{1}10]$ direction.

To determine the geometric structure of the overlayer from the STM images, we measure the positions of the observed corrulation maxima. Of course, the maxima observed in the STM images do not *exactly* coincide with the atomic locations due to shifts in the location of dangling bonds relative to the surface atoms. We briefly discuss here the possible magnitude of such shifts. The most favorable case occurs for semiconductor surfaces in which the dangling bonds are located almost exactly above the atoms, such as the Si(111)7×7 surface. There, the maxima in the STM images are expected to give an accurate measure of the lateral positions of the atoms, with an uncertainty of about 0.1 Å. A less favorable case occurs for dimers or zigzag chains of atoms, such as the Si(100)2×1, Si(111)2×1, or GaAs(110)1×1 surfaces. There, the dangling bonds may be directed laterally away from the atoms, and we expect the state density to be shifted somewhat away from the atoms. The only system for which this shift has been computed is GaAs(110), for which the separation between atomic positions and state-density maxima is found to be less then 0.5 Å (Ref. 21). In general, these types of shifts are not expected to be much greater than the spatial extent of a dangling bond, which is 0.5–1.5 Å. We emphasize that these relationships between the corrugation maxima and the atomic positions apply only to *lateral* position (i.e., in the plane of the surface). In the *vertical* direction the relationship between atomic positions and corrugation amplitudes is much more uncertain, since the corrugation amplitudes are greatly affected by the (unknown) electronic properties of the surface and also by the details of the probe tip. Thus, we use the lateral position of the corrugation, but not its amplitude, in our structural analysis.

For our measurement of the position of the observed STM maxima, we first consider the location of maxima associated with the $Sb^{(Ga)}$ atoms. The registration of these atoms relative to the GaAs substrate has already been illustrated in Figs. 4 and 5. This type of measurement has been repeated for several different samples and probe tips. For the $[\bar{1}10]$ direction, averaging over three measurements performed with two different samples and probe tips, we find an average shift of 1.84 Å with an uncertainty (one standard deviation) of 0.18 Å. For the [001] direction, averaging over five measurements performed with four different samples and probe tips, we find an average value of 2.92 Å with an uncertainty of 0.25 Å. The direction of this shift is that of the As dangling bond.

Turning now to the location of the $Sb^{(As)}$ atoms, Figs. 6 and 7 provide their positions relative to the $Sb^{(Ga)}$ atoms. For the [001] corrugation, we see in Fig. 6(c) a shift of about 2.8 Å (which corresponds to 0.5 unit cell) between $Sb^{(As)}$ and $Sb^{(Ga)}$ maxima. However, the $Sb^{(Ga)}$ maxima in Fig. 6(c) are themselves shifted by about 0.7 Å relative to the maxima in Figs. 6(a) and 6(b). This shift is attributed to the electronic properties of the surface, and it illustrates the overall uncertainty in the relationship between the STM images and the atomic locations. In Fig. 7 we also find a shift of about 2.8 Å between the [001] corrugations of $Sb^{(As)}$ and $Sb^{(Ga)}$ atoms. We have never observed any $[\bar{1}10]$ corrugation along the rows of $Sb^{(As)}$ atoms, and thus we cannot determine the location of these atoms in the $[\bar{1}10]$ direction.

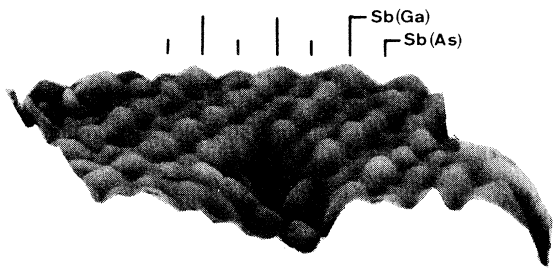

FIG. 7. Perspective view of a Sb terrace with the sample at -0.9 V. The image extends over a lateral area of approximately 45×25 Å^2.

C. Structural models

Using the relative positions of the various components of the corrugation determined in the preceding subsection, we now compare our results with models for the surface structure. In Fig. 8 we show four structural models, previously studied by LEED analysis,[4] along with a summary of our experimental results. In the figure the dashed rectangles outline a unit cell of an unbuckled GaAs surface. The model positions of the As and Ga atoms beneath the Sb overlayer are shown by solid and open circles, respectively, and the model positions of the Sb atoms are shown by the heavy open circles. The experimental results for the location of the Sb atoms are shown by the hatched areas. All of the coordinates in the figure repeat periodically to subsequent unit cells.

It is convenient in Fig. 8 to show the experimental results relative to an unrelaxed GaAs surface, whereas the measurements described above were performed relative to a relaxed (buckled) surface. We correct for this difference by shifting the observed [001] Sb corrugations by 0.42 Å, which is a theoretical result for the [001] shift of the As state-density maxima between a buckled and unbuckled surface.[21] The lateral extent of the hatched regions in Fig. 8 depict the uncertainty in our structural determination arising from the differences between the atomic locations and the positions of the maxima in the STM images. We use an uncertainty of ±0.8 Å, which falls in the middle of the estimated range of uncertainties discussed in Sec. III B. For the $Sb^{(As)}$ atoms, we were not able to observe their lateral position in the $[\bar{1}10]$ direction, and thus that uncertainty extends over the entire unit cell.

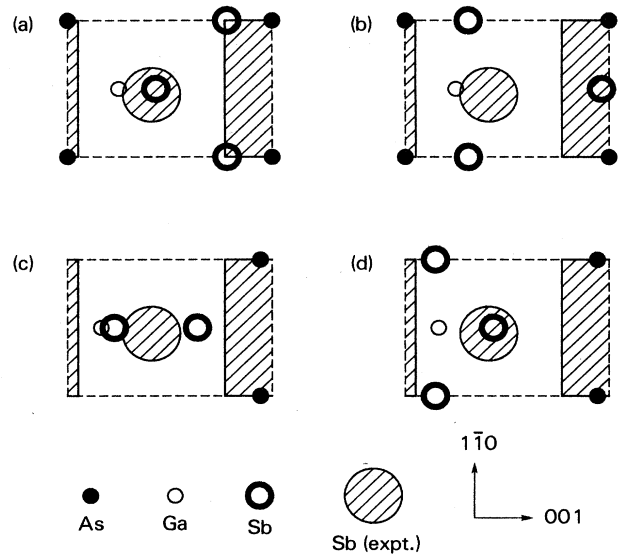

FIG. 8. Comparison of the spatial locations of the topographic features observed in the STM images with the positions of the two inequivalent Sb atoms for various structural models as given by the best-fit geometries according to the LEED analysis in Ref. 4. The unit cell of the *ideal* clean surface is shown by the dashed rectangle [for (a) and (b) the lateral positions of the Ga and As surface atoms are the same as the ideal positions, whereas for (c) and (d) they are relaxed from the ideal positions]. The data from the present experiment are shown as the hatched symbols, with the extent indicating the uncertainty as discussed in the text. We refer to the models as (a) bridging chain, (b) overlapping chain, (c) dimer, and (d) p^3.

We are now in a position to compare our experimental results with the structural models. We take the descriptions and coordinates of the models directly from a LEED analysis of this surface.[4] First, we consider the "bridging-chain model" shown in Fig. 8(a), in which the Sb atoms form zigzag chains bridging the GaAs chains of a nearly unreconstructed GaAs(110) substrate. The Sb atoms are then approximately located at the positions that would be occupied by Ga and As atoms in an additional GaAs layer. This model is the same as that shown in Fig. 1, and is the best structural candidate from the LEED analysis. As shown in Fig. 8(a), we find good agreement between experiment and model for both the $Sb^{(Ga)}$ and $Sb^{(As)}$ locations, although the latter lies near the edge of our estimated uncertainty range. Second, we consider the "overlapping-chain model" in which the Sb adatoms still form zigzag chains, but the chains are located directly on top of the GaAs chains of a nearly unrelaxed substrate. Bonding between the Sb and GaAs chains is accomplished via diffuse π bonding. As shown in Fig. 8(b), we find disagreement between experiment and model for the [$\bar{1}$10] corrugation location of $Sb^{(Ga)}$ atoms. Third, we consider the "dimer model" consisting of Sb_2 dimers bonding to the empty dangling bonds of the Ga atoms on a relaxed GaAs(110) substrate. As shown in Fig. 8(c), we find poor agreement for the locations of the [001] corrugation for both Sb atoms. Finally, we consider the "p^3 model" which consists of zigzag chains of Sb atoms on a relaxed substrate, with p^3 bonding both within the chain and between the chains and the substrate. As shown in Fig. 8(d), we find good agreement for the position of the $Sb^{(Ga)}$ atoms, while the agreement for the $Sb^{(As)}$ atoms is slightly outside of our estimated uncertainty range.

In summary, we find a best fit between experiment and model for the bridging-chain model, and a second best fit for the p^3 model. In the latter case, the LEED analysis gives a very poor fit,[4] so we conclude that the best structural candidate is the bridging-chain model pictured in Figs. 1 and 8(a). One additional structural model considered in the LEED analysis is a "defect model" consisting of only one Sb atom per unit cell. This model is inconsistent with our experimental results on ordered terraces where we observe (at low voltages) two Sb atoms per unit cell. However, the possibility of one Sb atom per unit cell existing on disordered parts of the surface is further discussed in the next section.

D. Hole defects

The Sb overlayers we observe in the STM images are not perfectly ordered. When less than a full monolayer of Sb is deposited, terraces form, bounded by a monoatomic step at the terrace edge. On top of the terraces excess Sb sometimes forms small protrusions, and within the terraces small holes or vacancies appear. These vacancies extend over one, a few, or many unit cells. Often, we find that the apparent depth of these vacancies as seen in the images is much less than the distance to the GaAs substrate. This effect is illustrated in Fig. 3(b), where we show two cross-sectional cuts through the STM image. In the image, dark-grey areas are seen, intermediate in height between the black GaAs and the light-grey Sb terrace. In the cuts, these intermediate areas are marked by the vertical lines located 0.6 Å below the ordered Sb.

We observe areas of intermediate height not only in the middle of terraces, but also at the edge of the terraces (as can be seen, for example, surrounding the GaAs part of Fig. 3). In principle, this sort of intermediate-height regions can be due to "ghost images" arising from tunneling to a secondary portion of the probe tip. In the present case, however, a close examination of the images reveals that these regions are seen near some terrace edges but not at others (with nominally the same orientation), thereby indicating that it is not a tip-convolution effect. The intermediate-height regions can extend over many unit cells, and in a few cases we can faintly resolve some corrugation within these regions.

We suggest here one possible origin of the vacancies and edge regions, namely that they arise from a half-monolayer coverage of Sb on the GaAs. Whereas the ordered terraces consist of two Sb atoms per unit cell, a half-monolayer coverage would contain one Sb atom per unit cell. It is unclear how such a species would bond to the substrate, although it seems probable that the vertical distance to the substrate would be less than that of the ordered overlayer. In a separate work, we have observed unique spectroscopic results which occur only at the

edges of the Sb terraces.[17] The half-monolayer Sb coverage discussed here would form one possible structural model to use in a theoretical description of the terrace edges.

E. Spectroscopy

For our spectroscopy studies of the surface-state density with the STM, we have used a new method which yields high-quality spectra with a large dynamic range. This method is principally useful for systems which display a large surface-state band gap, in which case conductivity measurements over 3–4 orders of magnitude are required to properly define the band edges and probe the gap region for the existence of states. We obtain this high dynamic range by varying the tip-sample separation as a function of voltage. We apply a continuous linear ramp to the tip-sample separation, moving the tip towards the surface as the magnitude of the voltage is reduced. The total variation in the tip-sample separation over a spectrum is typically in the range 4–6 Å.

Our data-acquisition method is illustrated in Fig. 9. In Figs. 9(a) and 9(b) we show raw data for the conductivity and current, as a function of voltage, obtained from a well-ordered region of the Sb overlayer. In the spectra we find a well-defined band gap in the region −0.4 to 1.0 V, along with some distinct spectral features on either side of the gap. The relative tip-sample separation, as a function of voltage, is shown in Fig. 9(c). To normalize the conductivity data, we take the ratio of dI/dV to I/V. The resultant "normalized conductivity" has been previously demonstrated to provide a measure of the state density which is approximately independent of tip-sample separation.[19,24]

For the present case of a system with a large surface-state band gap, we find that a significant problem enters into the normalization of the conductivity. Near the band edges, I/V generally approaches zero faster than dI/dV, so that the ratio of the two tends to diverge. This divergence is illustrated is Fig. 10(a), where we plot the ratio of dI/dV to I/V, computed directly from the data of Fig. 9. We see that the band edges (near −0.4 and 1.0 V) are not well defined. Also, $(dI/dV)/(I/V)$ is extremely noisy within the gap region, since I/V is close to zero. The origin of this problem can be seen by writing $dI/dV \propto \rho(\mathrm{eV})T(\mathrm{eV})$, where $\rho(\mathrm{eV})$ is the surface-state density and $T(\mathrm{eV})$ is a transmission factor. The role of I/V in the normalization is to provide an estimate of $T(\mathrm{eV})$. This estimate of $T(\mathrm{eV})$ is completely invalid in the gap region, in which the transmission itself does not approach zero. However, at sufficiently large voltages, I/V may still provide a meaningful estimate of $T(\mathrm{eV})$. We have found that a workable (albeit empirical) solution of this problem is to broaden the quantity I/V. The broadening is done with a one-pole Fourier low-pass filter, with the pole frequency given by ΔV^{-1}. In Fig. 9(d) we show I/V with no broadening, and with a broadening of $\Delta V = 1$ V.

In Fig. 10 we show results for the normalized conductivity, using various amounts of broadening ΔV. We emphasize that the differential conductivity dI/dV is *not* broadened—the procedure is only applied to the total conductivity I/V. Figure 10(a) shows the result using no

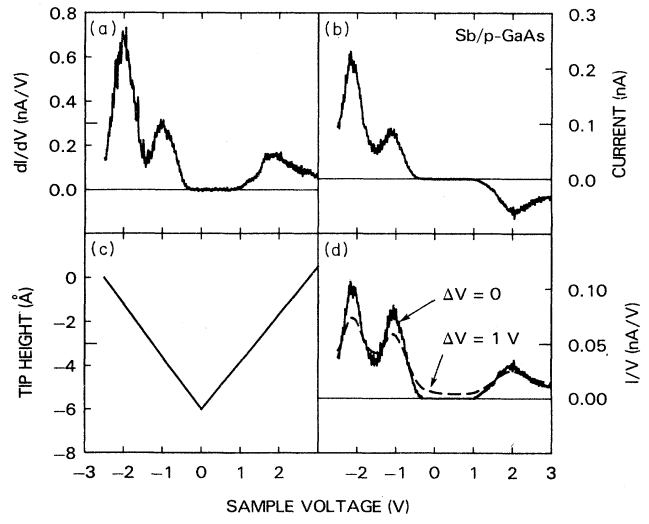

FIG. 9. Raw data for (a) the differential conductivity, and (b) the current, as a function of sample voltage. The applied variation in tip-sample separation is shown in (c). The total conductivity I/V is shown in (d), with no broadening (solid line) and a broadening of $\Delta V = 1$ V (dashed line).

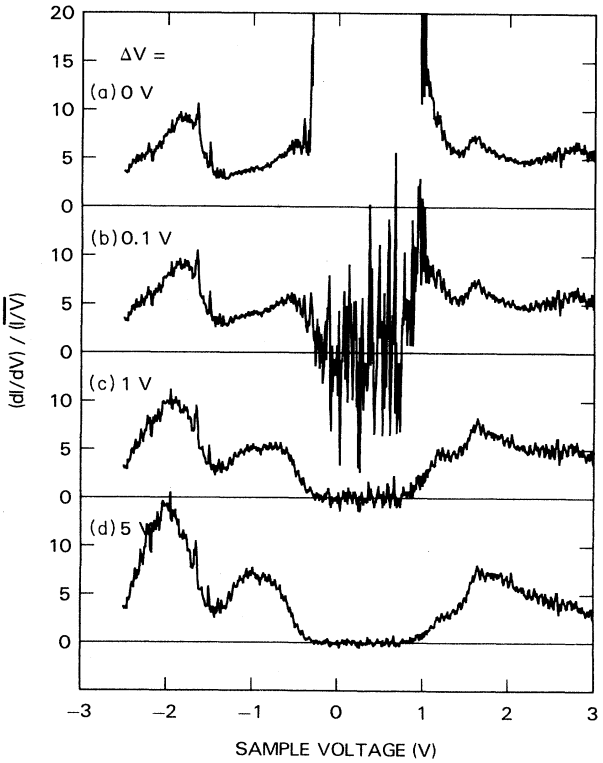

FIG. 10. Normalization of the conductivity spectrum (from Fig. 9), where I/V is broadened by various amounts ΔV. In curve (a) the normalized data become extremely noisy near 0 V, and that section of the curve is not plotted.

broadening, $\Delta V=0$ V, and Figs. 10(b)–10(d) show results for $\Delta V=0.1$, 1, and 5 V, respectively. We see that, with some broadening, the band edges become well defined, forming a band-gap region with normalized conductivity close to zero. The spectral peaks themselves are slightly shaped by the normalization, but their positions do not significantly vary with different ΔV. The final spectrum, Fig. 10(d), bears a close resemblance to the raw data shown in Fig. 9(a). This resemblance is not accidental, since our choice of z ramp in the spectrum is one which tends to minimize the variation of I/V across the spectral range.

In Fig. 11 we display various spectra, all obtained from ordered regions of Sb terraces on p-type GaAs. Figures 11(a) and 11(c) were obtained from the same sample with the same probe tip, and the other spectra were obtained from different samples using different probe tips. The depth of the z ramp varies, with values of 6, 6, 4, and 6 Å for Figs. 11(a)–11(d), respectively. The normalization of the spectra is as described above, using broadening intervals in the range 1.0–1.5 V. All of the spectra show two peaks on the filled-state side ($V<0$), and a single peak on the empty-state side ($V>0$). The spectra display a band-gap region with zero conductivity. In Fig. 11 we center the observed band-gap region relative to a bulk gap of 1.43 eV, with bulk gap edges denoted by E_V and E_C (this relative positioning of observed gap and bulk gap is discussed in more detail below). The amplitudes of the observed peaks vary among the spectra, although their positions, relative to the band edges, are constant to within a few tenths of an eV. (The shifts in the absolute positions of the band edges are due to variations in the local band bending at the surface.) We find the average positions of $E_V-0.4$ eV and $E_V-1.4$ eV for the peaks on the filled-state side, and $E_V+2.0$ eV for the peak on the empty-state side.

In addition to the results shown in Figs. 10 and 11, we have tried various other normalization schemes on the spectra. In Fig. 12(a) we show a constant-z normalization, again applied to the data of Fig. 9. In this method we multiply the conductivity by $\exp(2\kappa\Delta z)$, where Δz is the known variation in tip-sample separation. We use $\kappa=0.85$ Å^{-1}, which is a typical value for the decay constant measured on this surface. The resulting normalized conductivity is then plotted on a logarithmic scale, Fig. 12(a). The detection limit shown in the figure corresponds to the noise level of our measurement, scaled by the same exponential factor. An advantage of this particular normalization method is that its effect on the data is quite straightforward, although a disadvantage is that small features in the spectra are difficult to see on the logarithmic scale.

Another normalization scheme is shown in Fig. 12(b).

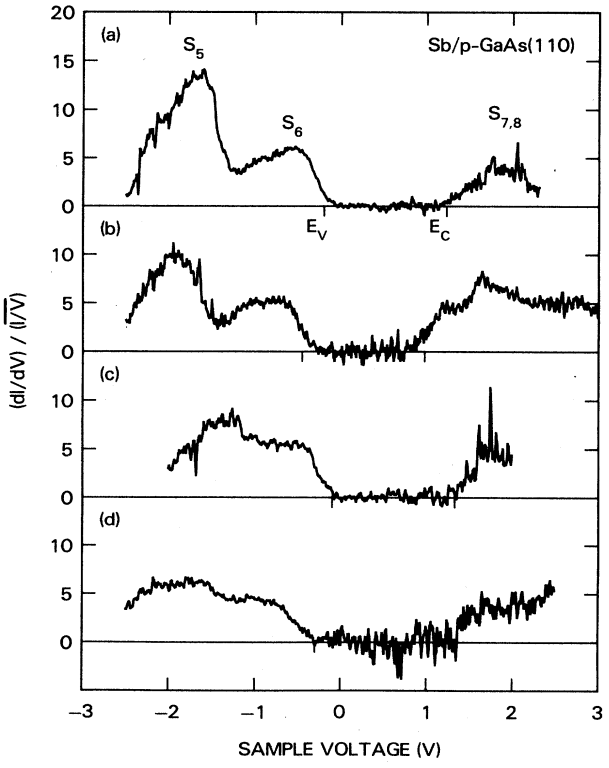

FIG. 11. Normalized conductivity vs voltage, obtained on Sb terraces on p-type GaAs(110). Spectra (a) and (c) were obtained from the same sample, and other spectra were obtained from different samples. The valence-band maximum (E_V) and conduction-band minimum (E_C) are indicated by tic marks.

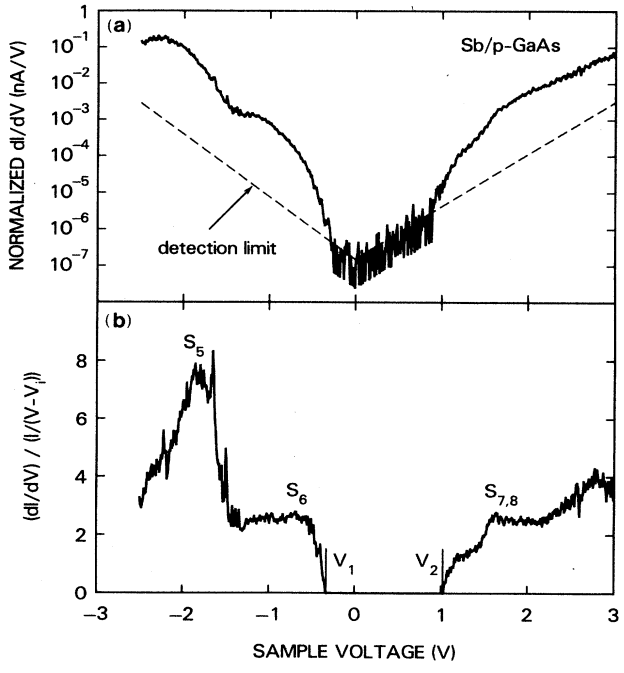

FIG. 12. Other normalization schemes for the spectral data: (a) exponential normalization to constant z, and (b) normalizing the conductivity to the quantity $I/(V-V_i)$, where V_i, $i=1,2$, are the onsets of the conductivity on either side on the band gap.

There, we again normalize the conductivity to the current. But then, rather than multiplying that quantity by V as in Fig. 10(a), we multiply by $V-V_i$, where V_i, $i=1,2$, are the onsets of the conductivity on either side of the band gap. Use of this modified form for the voltage multiplier eliminates the divergence problem discussed above while avoiding the procedure of broadening the current. The resultant spectrum is shown in Fig. 12(b). For this particular spectrum, we have $V_1=-0.33$ V for the filled states and $V_2=1.02$ V for the empty states. This procedure constrains the spectrum to equal zero at the band edges, and the spectrum is undefined within the band-gap region. The spectral features seen in Fig. 12(b) can be compared with those of Fig. 11(b) (which come from the same raw data). We see essentially the same features in both cases, although in Fig. 12(b) the S_6 peak looks more like a plateau, and the $S_{7,8}$ peak is much reduced in size. Figure 12(b) probably gives the best representation of the surface-state density, although this normalization method is not completely general since it does not provide any results within the band gap.

Our results for the spectroscopy can be compared with photoemission results,[10,11,15] and theoretical calculations.[5,7] In angle-resolved photoemission,[10,11] two peaks are seen near the top of the valence band. These peaks are associated with the S_5 and S_6 surface-state bands. The behavior of these bands, as found both in photoemission and theoretically, is as follows: S_6 is clearly visible over the entire surface Brillouin zone (SBZ), dispersing downwards in energy with increasing wave vector. S_5 can be seen near the edge of the zone, located at slightly lower energy than S_6, while it is strongly resonant with bulk bands near the zone center. The average separation of these two surface-state bands is observed in photoemission to be about 1 eV. The position of the two bands is in good agreement with the observed positions of the two peaks on the filled-state side of our spectra, and thus we associate the observed peaks with the S_5 and S_6 bands, as labeled in Fig. 11(a). The precise shape of the tunneling spectrum is not expected to agree with that seen in angle-resolved photoemission, since the matrix elements for the processes are completely different.

In inverse photoemission, an empty state is observed, located 2.0 eV above the valence-band maximum.[15] This value is in agreement with theoretical predictions[5,7] for the energy of a surface state, S_7, at the center of the SBZ, although the dispersion observed in experiment and theory do not agree. A second state, S_8 is predicted to occur at an energy slightly above that of S_7. The positions of these two states are in good agreement with the spectral feature we observe at about 2.0 eV above the valence-band maximum, and we associate that feature with some combination of the S_7 and S_8 bands.

We now turn to the positions of the valence-band maximum (E_V) and conduction-band minimum (E_C) as seen in Fig. 11. In general, the size of a band gap observed in a tunneling spectrum may be smaller than that in the bulk due to the occurrence of surface states within the bulk band gap. This is clearly seen, for example, for the Si(111)2×1 surface.[18,20] The observed gap will not be larger than the bulk gap as long as sufficient sensitivity is available in the measurement. For the case of the Sb overlayers, we find an observed gap which is very close in size to the bulk gap of 1.43 eV, as shown in Fig. 11. In some spectra the conductivity appears to extend into the gap region by 0.1 or 0.2 eV, possibly indicating that surface states extend into the bulk gap by this small amount. For comparison, angle-integrated photoemission finds 0.3 eV band bending for ordered Sb overlappers on *p*-type substrates, thus establishing an *upper limit* of 0.3 eV for the extent of the occupied surface state into the gap region.[14] As indicated above, inverse photoemission finds the empty states to lie outside of the gap region.[15] These experimental results are in good agreement with the tunneling spectra observed here, and confirm that the gap we observe in the tunneling spectra is practically coincident with the bulk band gap.

Finally, we return to the voltage-dependent imaging of Sec. III B, and consider those results in terms of the observed tunneling spectra. At large negative voltages (-2 to -3 V) we found that the Ga-bonded Sb atoms $Sb^{(Ga)}$ was seen. At small negative voltages (-1.5 to -0.9 V) the As-bonded Sb atom $Sb^{(As)}$, also appears, although it has a smaller amplitude than that of the Ga-bonded Sb atom. The nature of the surface state bands is known from theoretical considerations:[5,7] the S_5 band occurring at large negative energies consists mainly of As-bonded Sb character, whereas the S_6 band occurring at small negative energies consists mainly of Ga-bonded Sb character. The tunneling current integrates over a window of states, with the tunneling matrix element always favoring higher-lying states.[20] This selection is consistent with the STM images, in which we mainly observe the Ga-bonded Sb atom associated with the higher-lying S_6 state. The fact that we see *both* atoms at small negative voltages may be due to that fact that at those energies we are probing states near the center of the surface Brillouin zone, and these states have significant weight on both Sb atoms in the unit cell.

IV. SUMMARY

In summary, we have used the scanning tunneling microscope to study the geometric and electronic properties of antimony overlayers on the GaAs(110) surface. The Sb is observed to grow as a 1×1 ordered monolayer. The position of the Sb atoms in the unit cell has been deduced from voltage-dependent imaging. These positions are compared with various models for the surface structure, and a best fit is found for a model in which the Sb atoms form zigzag chains that bridge the GaAs chains on a nearly unrelaxed GaAs(110) substrate. The surface-state density has been measured with tunneling spectroscopy. A new spectroscopic method is used here, which enables us to obtain the entire spectrum, in a single scan, with high dynamic range. The normalization of the conductivity spectrum is discussed, and a method is introduced which overcomes some difficulties associated with large

band gaps. A band-gap region is observed in the tunneling spectra, with width nearly equal to the bulk band gap. Two distinct spectral features are seen on the filled-state side, and we associate these features with the S_5 and S_6 surface-state bands. On the empty-state side we see one broad spectral peak, which we associate with some combination of the S_7 and S_8 surface-state bands.

ACKNOWLEDGMENTS

It is a pleasure to thank R. Ludeke for many valuable discussions and A. P. Fein for expert technical assistance. We also thank J. Stroscio and R. Becker for numerous discussions relating to the spectroscopic methods used in this work.

[1]For a review, see L. J. Brillson, Surf. Sci. Rep. **2**, 123 (1982).

[2]P. Skeath, C. Y. Su, I. Lindau, and W. E. Spicer, J. Vac. Sci. Technol. **17**, 874 (1980); P. Skeath, I. Lindau, C. Y. Su, and W. E. Spicer, *ibid.* **19**, 556 (1981); P. Skeath, C. Y. Su, W. A. Harrison, I. Lindau, and W. E. Spicer, Phys. Rev. B **27**, 6246 (1983).

[3]J. Carelli and A. Kahn, Surf. Sci. **116**, 380 (1982).

[4]C. B. Duke, A. Paton, W. K. Ford, A. Kahn, and J. Carelli, Phys. Rev. B **26**, 803 (1982).

[5]C. M. Bertoni, C. Calandra, F. Manghi, and E. Molinari, Phys. Rev. B **27**, 1251 (1983).

[6]J. R. Myron, J. Anderson, and G. J. Lapeyre, in *Proceedings of the Seventeenth International Conference on the Physics of Semiconductors, San Francisco, 1984,* edited by D. J. Chadi and W. A. Harrison (Springer, New York, 1985).

[7]C. Mailhiot, C. B. Duke, and D. J. Chadi, Phys. Rev. Lett. **53**, 2114 (1984); Phys. Rev. B **31**, 2213 (1985).

[8]M. Mattern-Klosson and H. Lüth, Solid State Commun. **56**, 1001 (1985); M. Mattern-Klosson, R. Strümpler, and H. Lüth, Phys. Rev. B **33**, 2559 (1986).

[9]K. Li and A. Kahn, J. Vac. Sci. Technol. A **4**, 958 (1986).

[10]A. Tulke, M. Mattern-Klosson, and H. Lüth, Solid State Commun. **59**, 303 (1986).

[11]P. Mårtensson, G. V. Hansson, M. Lähdeniemi, K. O. Magnusson, S. Wiklund, and J. M. Nicholls, Phys. Rev. B **33**, 7399 (1986).

[12]W. Pletschen, N. Esser, H. Münder, D. Zahn, J. Guerts, and W. Richter, Surf. Sci. **178**, 140 (1986).

[13]R. Strümpler and H. Lüth, Surf. Sci. **182**, 545 (1987).

[14]F. Schäffler, R. Ludeke, A. Taleb-Ibrahimi, G. Hughes, and D. Rieger, Phys. Rev. B **36**, 1328 (1987); J. Vac. Sci. Technol. B **5**, 1048 (1987).

[15]W. Drube and F. J. Himpsel, Phys. Rev. B **37**, 855 (1988).

[16]1 ML corresponds to two Sb atoms per unit cell of the GaAs(110) surface, i.e., 8.85×10^{14} atoms/cm^2.

[17]R. M. Feenstra and P. Mårtensson, Phys. Rev. Lett. **61**, 447 (1988).

[18]R. M. Feenstra, W. A. Thompson, and A. P. Fein, Phys. Rev. Lett. **56**, 608 (1986); J. Vac. Sci. Technol. A **4**, 1315 (1986).

[19]J. A. Stroscio, R. M. Feenstra, and A. P. Fein, Phys. Rev. Lett. **57**, 2579 (1986).

[20]R. M. Feenstra, J. A. Stroscio, and A. P. Fein, Surf. Sci. **181**, 295 (1987).

[21]R. M. Feenstra, J. A. Stroscio, J. Tersoff, and A. P. Fein, Phys. Rev. Lett. **58**, 1192 (1987).

[22]P. Mårtensson and R. M. Feenstra, in Proceedings of the Third International Conference on Scanning Tunneling Microscopy, Oxford, 1988 [J. Microsc. (to be published)].

[23]J. A. Stroscio, R. M. Feenstra, D. M. Newns, and A. P. Fein, J. Vac. Sci. Technol. A **6**, 499 (1988).

[24]N. D. Lang, Phys. Rev. Lett. **34**, 5947 (1986).

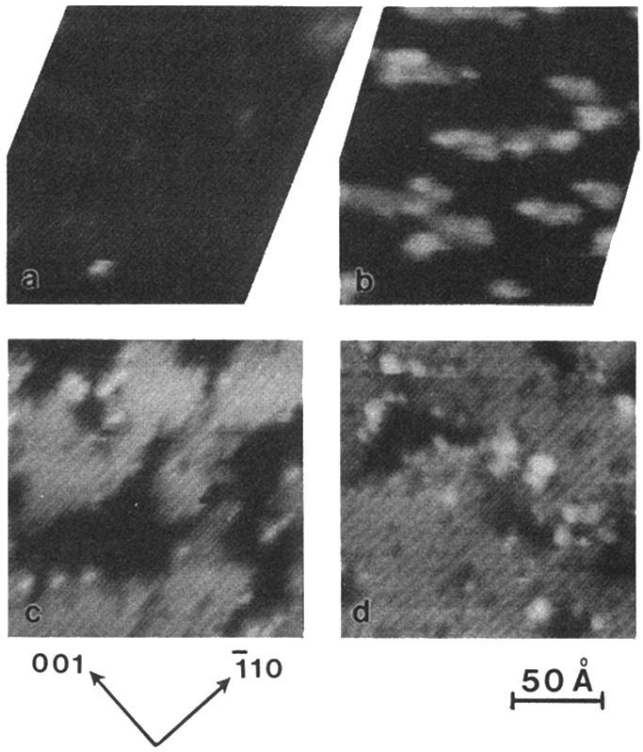

FIG. 2. STM images of GaAs(110) surfaces with increasing amounts of Sb. The coverages are (a) 0.03, (b) 0.2, (c) 0.7, and (d) 1.0 ML. The sample voltage was -2.5 V for images (a)–(c) and -2.0 V for image (d). The topographic height is displayed by a grey scale, ranging from 0 (black) to 6.5 Å (white).

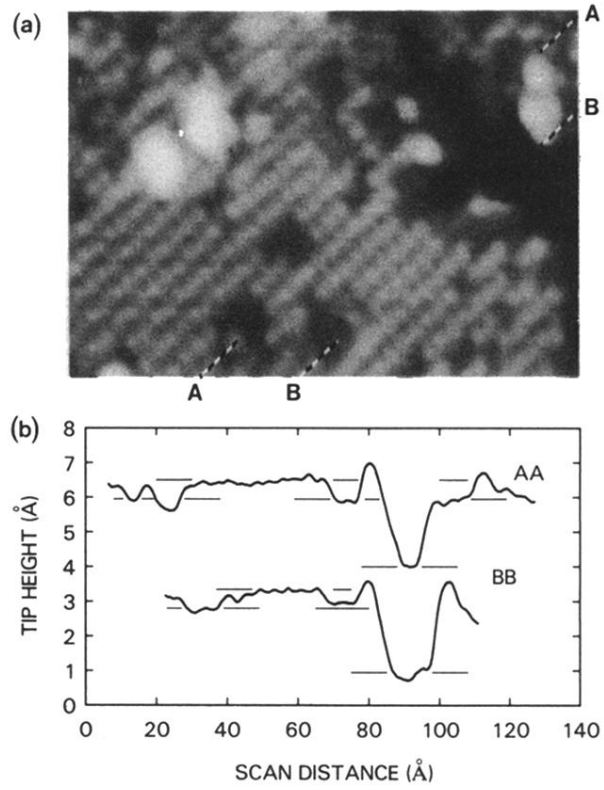

FIG. 3. (a) (120×90)-Å^2 STM image of antimony on the GaAs(110) surface, acquired with a sample voltage of −2.0 V. The Sb coverage is 1.0 ML. The topographic height is displayed by a grey scale, ranging from 0 (black) to 5 Å (white). (b) Cross-sectional cuts along the [$\bar{1}$10] direction, through the rows indicated in the image.

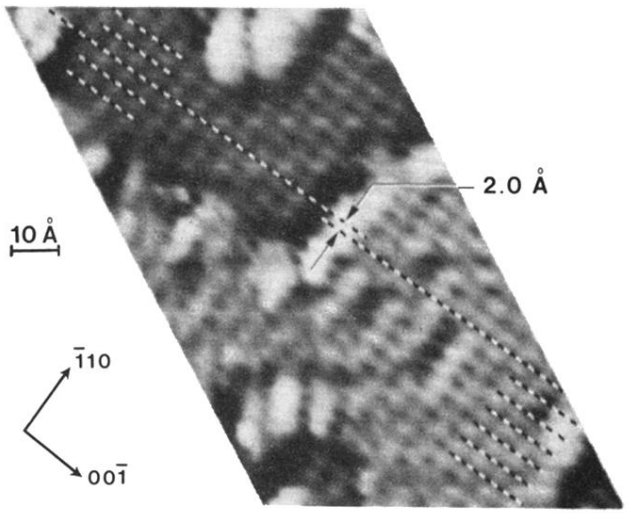

FIG. 4. STM image of the GaAs(110) surface covered with 0.7 ML Sb, acquired at a sample voltage of -2.0 V. The dashed lines are drawn through the minima of the $[\bar{1}10]$ corrugation, showing the registration of the Sb atoms with respect to the substrate As atoms.

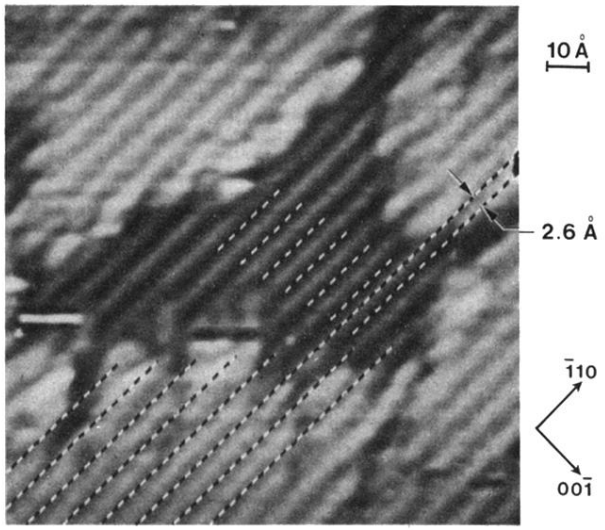

FIG. 5. STM image of the GaAs(110) surface covered with 0.7 ML Sb, acquired at a sample voltage of -2.5 V. The dashed lines are drawn through the minima of the [001] corrugation, showing the registration of the Sb atoms with respect to the substrate As atoms.

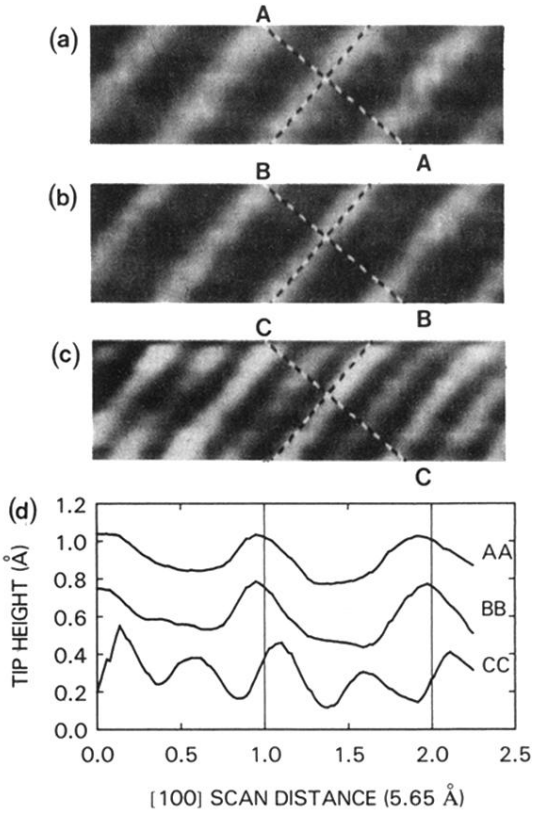

FIG. 6. (30×10)-Å^2 STM images of an ordered part of a Sb terrace acquired simultaneously at (a) −2.5, (b) −2.0, and (c) −1.5 V sample voltage. The crosshairs are located in identical positions in all images. The topographic height is displayed by a grey scale, ranging from 0 (black) to 0.5 Å (white). (d) Cross-sectional cuts along the [100] direction in images (a)–(c).

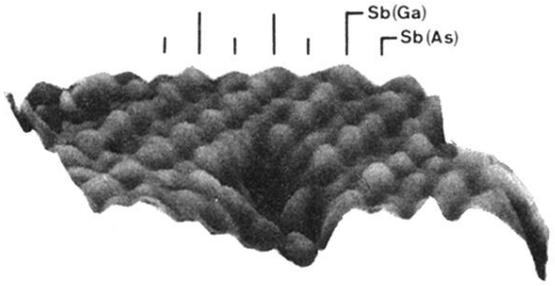

FIG. 7. Perspective view of a Sb terrace with the sample at −0.9 V. The image extends over a lateral area of approximately 45×25 Å^2.